ANOMALY DETECTION IN POST FIRE ASSESSMENT

Mihai Coca[1,2], *Mihai Datcu*[1,3]

[1]Research Center for Spatial Information (CEOSpaceTech), University POLITEHNICA of Bucharest (UPB)
[2]Computer Science and Cyber Security Laboratory, "Ferdinand I" Military Technical Academy
[3]Earth Observation Center (EOC), German Aerospace Center (DLR)

IGARSS 2021 - 2021 IEEE International Geoscience and Remote Sensing Symposium | 978-1-6654-0369-6/21/$31.00 ©2021 IEEE | DOI: 10.1109/IGARSS47720.2021.9554169

ABSTRACT

Over the last few years, natural disasters elevated dangerously in terms of immensity and prevalence over areas covered by forest and urban woodlands. Fast-spreading nature of the wildfires determine quick uncontrollable situations, causing significant effects in short periods. Despite increased difficulty in image processing approaches due to temporal resolution, complexity of spectral bands and illumination conditions, imagery data streams available from sun-synchronous satellites provide geospatial intelligence in monitoring and preventing fire threats. In this paper, we proposed a local scale burned area estimation framework that employs multispectral images in a deep learning architecture for detecting burned surfaces at patch level. This goal is accomplished by using an autoencoder (AE) network in which the latent feature layer learns normal background distribution, beneficial to background reconstruction. Furthermore, an outlier detection method (OCSVM) is used with aggregated features, latent and covariance components, in order to estimate burned coverage. Our method operates on data retrieved from Sentinel-2 (S2) constellation streaming source, which mainly contain normal scenes and limited fire affected spots.

Index Terms— Deep Learning, Anomaly Detection, Wildfires, OCSVM, Burned Area Estimation, Sentinel-2.

1. INTRODUCTION

Wildfires are a major factor for climate change and have a risk degree related to a number of factors, including temperature, soil moisture and presence of potential fuels (*e.g.* trees, shrubs). Climate variability creates warmer, drier conditions and a longer fire season due to more drier forest fuels. These volatile conditions impose an early wildfires detection system, capable to minimize the people' suffering and to maximise the time available for local authorities to intervene. Burned area estimates contribute in accurate spatial representation of fire expansions and perimeters. Precise plans of the burned areas are essential for recovery planning, calculating economic and environmental cost of fires and for gas and emissions estimations [1].

Majority of wildfire monitoring platforms rely on NASA MODIS (Moderate Resolution Imaging Spectroradiometer) imagery for burned area estimation, with the sensor centred at nadir and providing regional overviews as snapshots several times daily [2], but with a disadvantage for its relatively low spatial resolution. The European Forest Fire Information System (EFFIS) operates on daily satellite imagery from the MODIS sensor on board the TERRA and AQUA satellites. The EFFIS Rapid Damage Assessment module (RDA) provides daily update of the perimeters of burnt areas in Europe for fires of about 30 ha or larger, twice every day. The access on high availability of free medium-high spatial resolution optical satellite data has enabled the detection of fires below the 30 ha threshold. The advent of Multi Spectral Instrument (MSI) sensor aboard S2 satellites, equipped with specific spectral bands to record data in the vegetation red-edge spectral domain, allowed for the development and application of new spectral indices to discriminate and detect burned areas [3].

Traditional anomaly detection methods focus on spectral and spatial discrimination, as spectral signatures of anomalies are quite distinguishable in the spectral domain, surfacing small spatial footprints. Beyond these conventional approaches, statistical models using multivariate Gaussian distribution [4], representation-based detector like collaborative representation [5], deep neural network-based anomaly detection models capture more salient characteristics on satellite data than traditional techniques [6]. High-level semantic content of remote sensing images are modeled through advanced improvements in the field of deep learning. Methods based on deep neural networks are able to exploit the hierarchical or latent structure that is usually implicit to data through distributed feature representations. Deep learning applications with data access on massive remote sensing datasets need huge amount of annotated remote sensing images to conduct diverse EO monitoring, from crop supervising to risk and damage assessment [7].

Semi-supervised and unsupervised methods are predominantly employed in anomaly detection problems, in first case using a pretrained model trained with data containing only normal samples and second case employing a model more applicable for samples that are limited and difficult to obtain.

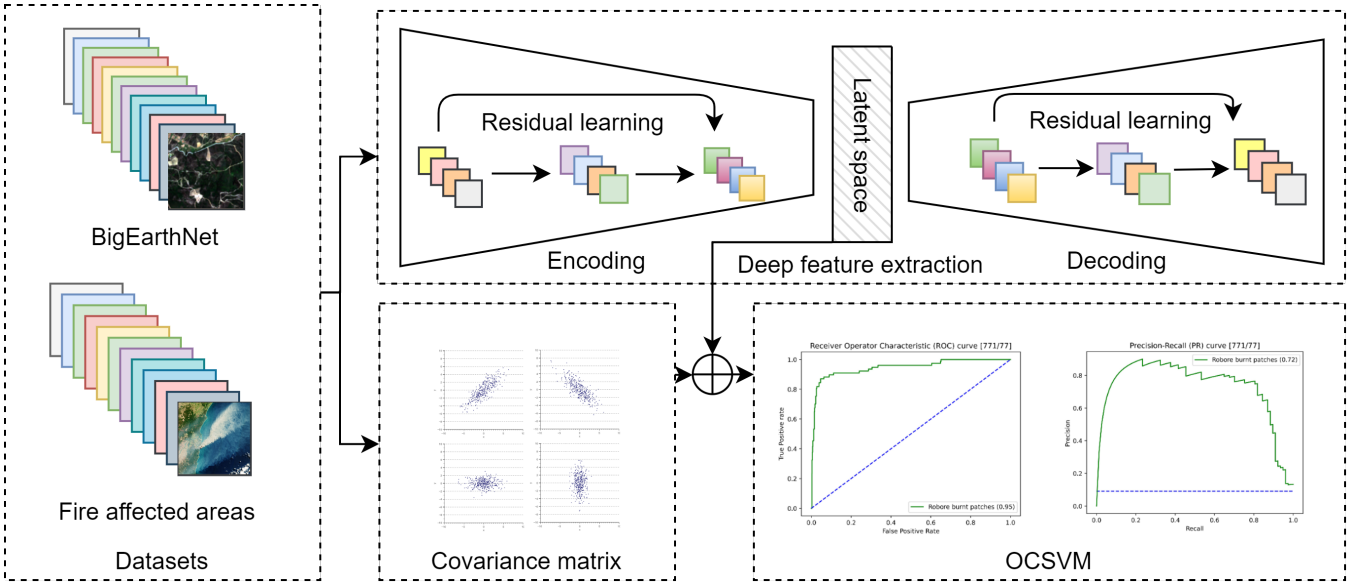

Fig. 1. Overview of the proposed framework that consists of tree modules: deep feature extraction, covariance matrix feature and OCSVM outlier detector.

Attractive deep learning-based methods such as autoencoder (AE) and generative adversarial networks (GANs), the former mainly as a preprocessor for detection and the latter as a generator of new data distribution with some new variations through a zero-sum game are broadly adopted in anomaly detection methodologies. Autoencoders computes reconstruction errors between the restored and the original input image. Anomalies are expected to have large reconstruction errors, while background has small reconstruction errors [8].

This work proposes a framework that detects and estimates anomalies in S2 data based on the potential of AE reconstruction ability. The contribution of this work is concentrated on defining a methodology for estimating a particular anomaly kind, specifically fire affected vegetation through multispectral S2 imagery. The remainder of this paper is organized into four sections. In Section II, relevant works are discussed in the context of wildfire detection and post fire evaluation. Section III introduces necessary information about the proposed framework. The experimental results of our proposed method are presented in Section IV. Section V draws the conclusion.

2. RELATED WORK

In literature, a common procedure to highlight burned regions is the use of indices computed from the combination of satellite spectral bands. In [9], a burned area index (BAIS2) specifically defined for S2 acquisitions is proposed to perform post-fire mapping using S2 data. A change detection procedure using dense S2 time series with no a priori knowledge about wildfire occurrence or burned areas spatial distribution is described in [3]. Bi-temporal difference spectral indices, based on spectral indices and arithmetic differences between pre-fire and post-fire values, have been shown to provide better results compared to the methods based on a single temporal observation [9]. An aggregate procedure for data representation, feature extraction and feature classification is proposed in [10]. Authors shown that dimensionality reduction plays a key role in burned area mapping on S2 data.

In [11], authors introduced an unsupervised algorithm, Burned Area Estimation through satellite tiles (BAE), that automatically delineate the burned areas of wildfires from satellite imagery. Through merging image processing techniques and an unsupervised neural network, BAE method proved to overcome the limitation that a training set can not contains all possible conditions (e.g., land type, vegetation intensity).

Majority of burned area mapping methods depend on time series data (e.g. pre-fire and post-fire images) in order to generate a binary mask of the burned area. We aim to overcome the need of before-event image and detect from a single temporal observation the anomalous burned patches.

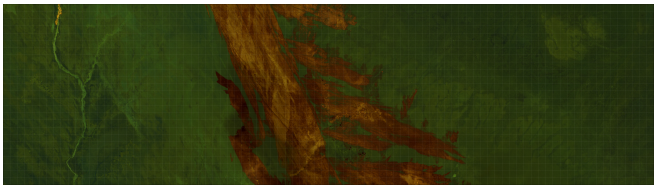

Fig. 2. S2 image, Robore, Bolivia, 23 August 2019. Pseudo-color representation for B12, B11 and B9 channels. Coordinates for upper left pixel are Lat $18°47'17''S$ Lon $60°09'15''W$.

3. METHODOLOGY

Residual learning is utilized to avoid the loss of weak information while deepening the network. To avoid degradation problem [12], our proposed framework heavily relies on ResNet [13] encoder-decoder architecture to extract salient features with capability of preserving representations from degrading. For feature extractor, we adopted a self-supervised learning approach to extract meaningful representations in the context of unlabeled data. We kept a symmetrical model for feature learning and exploit the encoder and its representation competence to a downstream anomaly detection task.

A flowchart of the proposed method is shown in Fig. 1. In inference phase, for each input patch, a covariance matrix is computed in order to be used as a strong spatial feature on downstream classification. The aim of the covariance measure is to determine the variability between each pair of input bands. The knowledge of how spectral channels vary together is concatenated to latent component in order to obtain the final feature vectors used in One-Class Support Vector Machine (OCSVM) training. The outlier detection model is trained using images of unaffected areas. Lastly, burned areas are detected by the trained OCSVM.

3.1. Model

An autoencoder first encodes the input tensor into a lower dimensional latent representation, then decodes the latent representation back to an resemblant tensor. The goal is to learn to compress the data while minimizing the reconstruction error. The reconstruction process of nonlinear mapping of feature x to itself follows two micro processes, the encoder, parameterized with h_e, that infers data representation z from input feature x

$$z = f(h_e(x))) \tag{1}$$

and the decoder, parameterized with h_d, that tries to reconstruct $\hat{x}$ from embedding z

$$\hat{x} = f(h_d(z))) \tag{2}$$

Loss function. We followed a valid baseline for a regression objective, and for optimization in data reconstruction. As the predicted variable is continuous, we implied the mean squared error $\mathcal{L}_2(\bullet, \bullet)$, as the loss function:

$$\mathcal{L}_2(x, \hat{x}) = \frac{\lambda}{n} \sum_{n,h,w,\delta} \|x_{n,h,w,\delta} - \hat{x}_{n,h,w,\delta}\|^2 \tag{3}$$

where λ is a weighting parameter and (n, h, w, δ) represents the input shape.

Training details. The feature extraction method was trained from scratch using ResNet-18 [13] backbone network for the encoder and its counterpart for decoder. We removed last linear layer from ResNet-18 architecture and adapted first layer for 12 channels input. After a dropout layer and 4 stacked sequential analogue layers, a sequence of an upsampling operation followed by a batch normalization layer, a ReLU activation, and a transposed convolution is added to the top of the decoder. In training process a fix learning rate at 0.01, 50 epochs and a small batch size equal to 64 are adopted. We chose value of 64 with the motivation that small batch training leads to flat local minimum, and hence better generalization. As preprocessing steps, a bicubic interpolation for channels with 20m and 60m resolution and a 16 bits normalization in $[0, 1] \in \mathbf{R}$ were implied.

3.2. Datasets

BigEarthNet [14] is a challenging large-scale multispectral dataset consisting of 590,326 image patches from the S2 satellite. This is a multi-label land-cover dataset with a highly unbalanced label distribution. Data was collected in a relatively short time period, covering all seasons. In the winter season, there is an lower cardinality of annotated images due to high percentage of cloud cover. As the performance of any deep learning model is directly proportional to the quality of input training data, 70,987 images that are fully covered by seasonal snow, cloud and cloud shadow have been eliminated from dataset. We used a random part from BigEarthNet dataset for training our model.

The tested dataset is a tile of 109,8x30 km^2 that sweeps a south area of Robore town, Bolivia. These data were acquired in 23 August 2019, when an ravage outbreak of wildfires was in place. We tiled this scene in non-overlapping image patches using same dimension as BigEarthNet (120x120 pixels for 10m bands, 60x60 pixels for 20m bands and 20x20 pixels for 60m bands). In Fig. 2 is shown in pseudo-color representation the region of interest. The Robore scene contains mostly *Chiquitano dry forest* flora, with a percentage of burned tiles (brownish colour) equal to $\sim$26% from a total of 2250 patches.

4. EXPERIMENTS

Quantitative results are reported using commonly Precision-Recall (PR) curve metric. In our experiment, we used 100000 patches from BigEarthNet dataset, sorted into a 60% training set to learn the parameters, a 20% validation set to monitor network overfitting state and 20% test set to assess the final prediction performance, on the side of feature extractor training.

No. of ab. patches	7	15-53	61	69-77
Anomaly in dataset [%]	0.9	1.94-6.8	7.9	8.9-9.9
AUPRC [0-1]	0.46	0.54-0.66	0.71	0.72

Table 1. Evolution of AUPRC based on anomaly quantity.

The training process of OCSVM implied only normal data, acquired entirely from BigEarthNet dataset. In order to vary a score threshold for reported metric into OCSVM instance, we computed the outlier scores using

$$score(x_i) = \max_x f(x) - f(x_i) \quad (4)$$

where x is the entire test set, x_i is the i-th test point and f is the decision function. OCSVM has a parameter ν that establishes the ratio of normal and abnormal areas. This trade-off between the false positive (abnormal) and false negative (normal) is empirically set to a fixed value of 0.7. This decision come from the homogeneity characteristic of the normal data.

We conducted an experiment using a test dataset containing 771 normal and 77 abnormal patches, from the left half of the scene in Fig. 2. This is an optimistic ratio in comparison with real world cases where anomalous samples exist in lower percentages. For this reason, we started with 0.9% abnormal data in test dataset and iteratively incremented with $\sim$0.9% until reaching the entire 77 available abnormal tiles. In Table 1 is highlighted the evolution of area under PR curve (AUPRC) based on the abnormal data percentage included in test dataset. Under 2% anomalous patches in dataset, the classifier is not able to distinguish between positive and negative class points. For 7.9%, an accuracy of 0.71 is achieved. One can observe the positive evolution of precision and recall factors for each anomalous patch extension.

5. CONCLUSION

In this study, a burned area detection algorithm using an autoencoder model and OCSVM for spectral images was designed. The residual autoencoder extracts deepen features from input data and the outlier detection model spots fire affected areas. The proposed approach demonstrated a consistent capability of anomaly detection in the context of fire affected areas in a particular scene.

For result improvement, a continuous development direction of our framework is to build a geographically independent model for estimating the S2 burned area, because locally developed algorithms are difficult to transfer to other regions due to differences in surface reflectance and backscatter coefficients. Development of a custom loss function may provide benefits in model performance, essentially when presence of shadows and great changes during summer and winter season change drastically the S2 spectral signature. Another gain may materialize through emphasizing the qualification of the SWIR bands in model construction as they are less influenced by scattering than the visible bands and are well associated to post-fire impacts.

6. REFERENCES

[1] A. K. Jain, "Global estimation of co emissions using three sets of satellite data for burned area," *Atmospheric Environment*, vol. 41, no. 33, pp. 6931 – 6940, 2007.

[2] L. Giglio, W. Schroeder, J. V. Hall, and C. O. Justice, "MODIS Collection 6 Active Fire Product User's Guide Revision B," December, 2018.

[3] F. Filipponi, "Exploitation of sentinel-2 time series to map burned areas at the national level: A case study on the 2017 italy wildfires," *Remote Sensing*, vol. 11, no. 6, pp. 622, 2019.

[4] B. Du and L. Zhang, "A discriminative metric learning based anomaly detection method," *IEEE TGRS*, vol. 52, no. 11, pp. 6844–6857, 2014.

[5] W. Li and Q. Du, "Collaborative representation for hyperspectral anomaly detection," *IEEE TGRS*, vol. 53, no. 3, pp. 1463–1474, 2015.

[6] R. Chalapathy and S. Chawla, "Deep learning for anomaly detection: A survey," *arXiv:1901.03407*, 2019.

[7] G. Cheng, J. Han, and X. Lu, "Remote sensing image scene classification: Benchmark and SoA," *Proceedings of the IEEE*, vol. 105, no. 10, pp. 1865–1883, 2017.

[8] A. Makhzani, J. Shlens, N. Jaitly, I. Goodfellow, and B. Frey, "Adversarial autoencoders," 2016, arXiv:1511.05644.

[9] F. Filipponi, "Bais2: Burned area index for sentinel-2," *Multidisciplinary Digital Publishing Institute Proceedings*, vol. 2, no. 7, pp. 364, 2018.

[10] A. Grivei, C. Văduva, and M. Datcu, "Assessment of burned area mapping methods for smoke covered sentinel-2 data," in *2020 13th International Conference on Communications (COMM)*, 2020, pp. 189–192.

[11] A. Farasin, G. Nini, P. Garza, and C. Rossi, "Unsupervised burned area estimation through satellite tiles: A multimodal approach by means of image segmentation over remote sensing imagery," in *MACLEAN@PKDD/ECML*, 2019.

[12] K. He, X. Zhang, S. Ren, and J. Sun, "Spatial pyramid pooling in deep convolutional networks for visual recognition," in *European Conference on Computer Vision*, 2014, vol. 8691, pp. 346–361.

[13] K. He, X. Zhang, S. Ren, and J. Sun, "Deep residual learning for image recognition," in *2016 IEEE Conference on Computer Vision and Pattern Recognition (CVPR)*, 2016, pp. 770–778.

[14] G. Sumbul, M. Charfuelan, B. Demir, and V. Markl, "Bigearthnet: A large-scale benchmark archive for remote sensing image understanding," in *IEEE IGARSS*, July 2019, pp. 5901–5904.